Electronic Supplementary Information†

An in-situ DNA content detection enabled by organic long-persistent luminescence materials with tunable afterglow-time in water and air

Man Liu,[‡a] Desissa Yadeta Muleta,[‡a] Zhenyi Yu,[a] Lichang Wang,[b] Dongzhi Liu,[c] Tianyang Wang*[a] and Wenping Hu*[ade]

Table of contents

1. Characterization data

Synthesis of new compound DDFy.

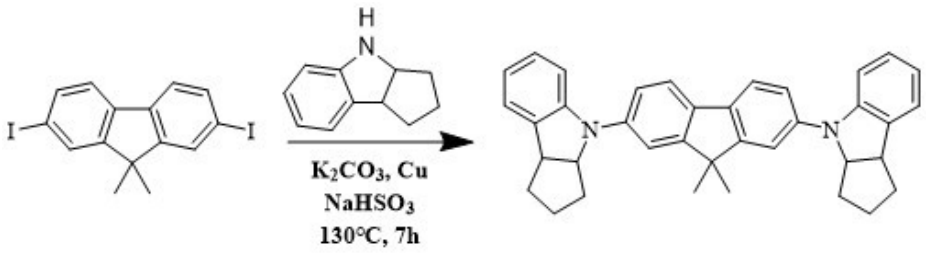

Scheme S1. Synthesis scheme of DDFy.

Structure characterization of DDFy. ^{1}H NMR ($CDCl_3$, 400 MHz) δ: 7.57 (d, J=8.0 Hz, 2H), 7.35 (s, 2H), 7.22-7.01 (m, 8H), 6.73 (s, 2H), 4.82 (s, 2H), 3.86 (s, 2H). 2.01-1.43 (m, 18H). ^{13}C NMR ($CDCl_3$, 100.6 MHz) δ: 151.18, 141.47, 133.18, 129.06, 127.12, 126.50, 124.82, 124.30, 119.66, 118.15, 114.97, 108.33, 63.17, 53.54, 47.26, 36.97, 34.99, 24.48, 18.47. HRMS (APCI): m/z = 508.2873 (M^+) (calcd for $C_{37}H_{36}N_2^+$: m/z = 508.2873). Elem. Anal.: Found: C, 87.47; H, 7.09; N, 5.44% (Calc. for $C_{37}H_{36}N_2$: C, 87.36; H, 7.13; N, 5.51%). ^{1}H NMR and ^{13}C NMR spectra were exhibited in Fig. S9, S10, ESI†.

Structure characterization of DDF. ^{1}H NMR ($CDCl_3$, 400 MHz) δ: 7.41 (d, J=8.0 Hz, 2H), 7.21-7.16 (m, 8H), 7.07-7.01 (m, 10H), 6.94-6.85 (m, 6H), 1.26 (s, 6H). ^{13}C NMR ($CDCl_3$, 100.6 MHz) δ: 153.94, 146.95, 145.55, 142.00, 128.29, 128.13, 122.87, 122.49, 121.42, 119.96, 118.96, 117.73, 116.76, 45.73, 26.03. HRMS (APCI): m/z = 528.2563 (M^+) (calcd for $C_{39}H_{32}N_2^+$: m/z = 528.2560). Elem. Anal.: Found: C, 88.69; H, 6.05; N, 5.26% (Calc. for $C_{37}H_{36}N_2$: C, 88.60; H, 6.10; N, 5.30%). ^{1}H NMR and ^{13}C NMR spectra were exhibited in Fig. S11, S12, ESI†.

Structure characterization of DDFp. ^{1}H NMR ($CDCl_3$, 400 MHz) δ: 8.18 (d, J=8.0 Hz, 4H), 7.99 (d, J=8.0 Hz, 2H), 7.68 (s, 2H), 7.61-7.59 (m, 2H), 7.51-7.43 (m, 8H), 7.34-7.30 (m, 4H), 1.62 (s, 6H). ^{13}C NMR ($CDCl_3$, 100.6 MHz) δ: 154.59, 139.87, 136.56, 135.87, 125.02, 124.95, 122.35, 120.43, 120.25, 119.34, 118.94, 108.75, 52.37, 46.36, 26.03. HRMS (APCI): m/z = 524.2242 (M^+) (calcd for $C_{39}H_{28}N_2^+$: m/z = 524.2247). Elem. Anal.: Found: C, 89.15; H, 5.40; N, 5.45% (Calc. for $C_{37}H_{36}N_2$: C, 89.28; H, 5.38; N, 5.34%). ^{1}H NMR and ^{13}C NMR spectra were exhibited in Fig. S13, S14, ESI†.

TGA. The thermal stability of the samples was determined by measuring the weight loss while heating at a rate of 10 ºC min^{-1} from 25 ºC to 600 ºC under inert nitrogen atmosphere.

DSC. The samples were heated at a rate of 10 ºC min^{-1} from 30 ºC to 300 ºC under inert nitrogen atmosphere.

CV. The electrochemical properties were measured using a BAS 100W electrochemical analyzer utilizing the three-electrode configuration with a glassy carbon electrode as the working electrode, $Ag/AgNO_3$ electrode as the reference electrode, and platinum as the auxiliary electrode. The analyzer was calibrated using a ferrocene/ferrocenium redox couple as the external standard prior to the measurements. The scan rate was set to 30 mV/s. Dichloromethane containing 0.1 $mol \cdot L^{-1}$ tetra-butylammoniumhexafluorophosphate ($TBAPF_6$) was employed as the medium for the cyclic voltammetric determination. The compound concentration was 5×10^{-4} $mol \cdot L^{-1}$.

TC-SPC. Sample excitation was done with picosecond diode lasers (Horiba Jobin Yvon Instruments) at 321 nm or 375 nm, and the time resolution was ~ 150 ps. The laser pulse energy was ca. 15 pJ and attenuated (often by more than an order of magnitude) to the desired count rate of ca. 1% or less of the excitation frequency. A cooled (ca. -40°C) Hamamatsu MCP- photomultiplier R3809U 51 was used for detection of single photons, and the signal passed through a discriminator (Ortec 9307) and into a TAC (Ortec 566, 100 ns range used). The electrical trigger signal from the laser was also passed through a discriminator (Tennelec TC454) and on to the TAC (Ortec 566). The TAC output was read by a DAQ-1 MCA computer card using 1024 channels and collected with Horiba Jobin Yvon Data Station 2.5. Measurements were made in reverse mode at 5 MHz and under magic angle polarization. A cut-off filter, GG400 (Excitation at 321 nm) or GG 515 (Excitation at 375 nm), was used to block stray excitation light. A dilute solution of Ludox was used to record the instrument response function without any filter for solution measurements. No monochromator was used, i.e. all wavelengths transmitted by the cut-off filter were collected.

Fs-TA. The laser pulses of the femtosecond transient absorption was generated by a Ti:sapphire femtosecond laser system. The mode-locked Ti:sapphire laser (Tsunami, Spectra Physics) delivered laser pulses at 800 nm (120 fs, 1 kHz) as a seed to the generative amplifier (Spitfire, Spectra Physics), and divided

then into two components. The major one was used to generate the pump pulses (370 nm, 130 fs, 1 kHz), and the minor to generate the probe pulses. The probe wavelength was selected by a band-pass filter. The time delay between the probe and pump beams was regulated using a computer-controlled motorized translation stage. The temporal resolution was determined to be about 150 fs and the transmitted light was detected by a linear image sensor (S8377-512Q, Hamamatsu). The 1 mm rotating sample cell was excited by 0.1 μJ/pulse. A typical absorbance at the excitation wavelength was 0.4−0.6.

HPLC. Methanol (MeOH) mixed with ultra-pure water was used as mobile phase and C_{18} was used as stationary phase. Samples were dissolved in MeOH/H_2O (v/v = 4:1) for a concentration of 1 mg·mL^{-1} and the injection volume was set as 10 μL. All the samples were filtered through a 0.45 μm membrane before usage. UV absorbance was detected at 254 nm. All the separations were performed with a flow rate of 1 mL·min^{-1} at 30 ºC.

Supplementary discussion of Fig. S5. Fluorescence emission of the DPA:DDF and DPA:DDFp crystals at 420 nm are modeled by bi-exponential decay. The major and fast component of fluorescence emission lifetimes, 1.0 ns (95%) for DPA:DDF and 1.0 ns (13%) for DPA:DDFp, are ascribed to the photo-induced electron transfer from the excited DDF (DDFp) to the DPA module to form the CS states. The minor and slow component of fluorescence emission lifetimes, 4.6 ns (5 %) for DPA:DDF and 13.0 ns (87 %) for DPA:DDFp, are attributed to the singlet-triplet conversion.[1-5] Meanwhile, fluorescence emission of the DPA:DDFy crystals at 420 nm has been modeled by mono-exponential decay with one lifetime of 1.0 ns, indicating that the conversion from DDFy singlets to DDFy triplets is almost through the charge separation process (~100%) rather than the traditional ISC process.

Traditional DPA colorimetric reaction method. DNA of different quality and a certain amount (27 mg·mL^{-1} of DPA aqueous solution) of the DPA reagent (Preparation: 4g of diphenylamine was dissolved in 100 mL of glacial acetic acid and 2.7mL of 98% concentrated sulfuric acid) were added into pure water for a constant volume and the mixture was then stirred at 70℃ for 1.5 h. Cooled the solution to room temperature and observed its color change. DNA qualitation and quantitation can be achieved by analyzing the typical absorbance of blue products of DPA colorimetric reaction at 595 nm.[6] Under acidic conditions, as one of the

hydrolyzed products of DNA, 2-deoxyribose released from purines (but not pyrimidines) can be further oxidized to 5-hydroxy-4-oxopentanal, and then dimerized as well as specifically condensed with DPA to obtain blue products.

2. Supplementary table and figures

Table S1. Some proven methods enable DNA content detection

Methods	Detection principles	DNA separation	In-situ detection	Limit of detection
Our method	Organic persistent-RTP / Organic long-persistent luminescence	No	Yes	46 μg·mL^{-1}
Diphenylamine colorimetric reaction[7]	UV-vis	Yes	No	10 μg·mL^{-1}
UV–vis spectrophotometry[8]	UV-vis	Yes	No	100 fM
Fluorescent probes[9]	Fluorescence	Yes	No	4.2 ng·mL^{-1}
Electrophoresis method[10]	Fluorescence	Yes	No	7.0 ng·mL^{-1}
ChemiLuminescence (CL) method[11]	Fluorescence	Yes	No	7.8 ng·mL^{-1}
Polymerase chain reaction (PCR) method[12,13]	Raman scattering / Fluorescence	Yes	No	12 aM; 100 fM
Electrochemical sensing method[14]	Redox reaction	Yes	No	1.3 aM
HPLC-MS/MS method[15]	HPLC-MS/MS	Yes	No	25 fM
Room-temperature phosphorescence (RTP) probes based on organic-inorganic hybrid system[16-18]	RTP	Yes	NO	0.5 pM; 1.5 pg·mL^{-1}; 19.48 ng·mL^{-1}

Table S2. The fluorescence and phosphorescence quantum yields of doped-crystals.

Sample	Φ(fl) (%)	Φ(ph) (%)
DPA:DDFy	64.8	35.5
DPA:DDF	54.7	28.4
DPA:DDFp	28.2	13.2

Table S3. Frontier orbital energies (HOMO and LUMO) and some energy level data upon excitation for DDF, DDFy, DDFp, and DPA. The energy of the CS states, DDF***x***$^{\bullet+}$-(DPA)$_n$-DPA$^{\bullet-}$ (E_{cs}, x = y, p or none), estimated by the offset of the electrochemically measured HOMO and LUMO energies (E_{cs} = -(E_{HOMO}^{DDFx}-E_{LUMO}^{DPA}), 2.8 eV for DDF$^{\bullet+}$-(DPA)$_n$-DPA$^{\bullet-}$ and DDFy$^{\bullet+}$-(DPA)$_n$-DPA$^{\bullet-}$, and 3.0 eV for DDFp$^{\bullet+}$-(DPA)$_n$-DPA$^{\bullet-}$), and the (DPA)$_n$ (n $\geqslant$ 0) refers to several DPA molecules.

Sample	HOMO[a)] (eV)	LUMO[b)] (eV)	λ_{max}(abs) (nm)	λ_{max}(fl) (nm)	E(S_1)[c)] (eV)	λ_{max}(ph) (nm)	E(T_1)[d)] (eV)
DDF	-5.1	-2.1	374	420	3.1	526	2.4
DDFy	-5.1	-2.1	381	437	3.0	522	2.4
DDFp	-5.3	-2.2	374	414	3.1	558	2.2
DPA	-5.7	-2.3	294	347	3.9	430	2.9

a) The HOMO energy was deduced from the oxidation onset potential from cyclic voltammetry data and calculated by the equation: E_{HOMO} = -E_{onset} - 4.93 (eV).

b) E_{LUMO}= E_{HOMO} + Eg_{op}, the optical band gap (Eg_{op}^{DDFx}, the value was 3.0 eV, 3.0 eV and 3.1 eV for crystals DDF, DDFy and DDFp, respectively; Eg_{op}^{DPA}, the value was 3.4 eV for crystal DPA) was estimated from the onset of the absorption band.

c) Singlet energies E(S_1) were calculated from absorption and fluorescence spectra of the crystals of DDF derivatives and DPA, that is, E(S_1) = 1241/[(λ_{abs}+λ_{fl})/2].

d) Triplet energies E(T_1) were due to phosphorescence spectra of the crystals of DDF derivatives and DPA with the formula E(T_1) = 1241/$\lambda_{ph.}$[19]

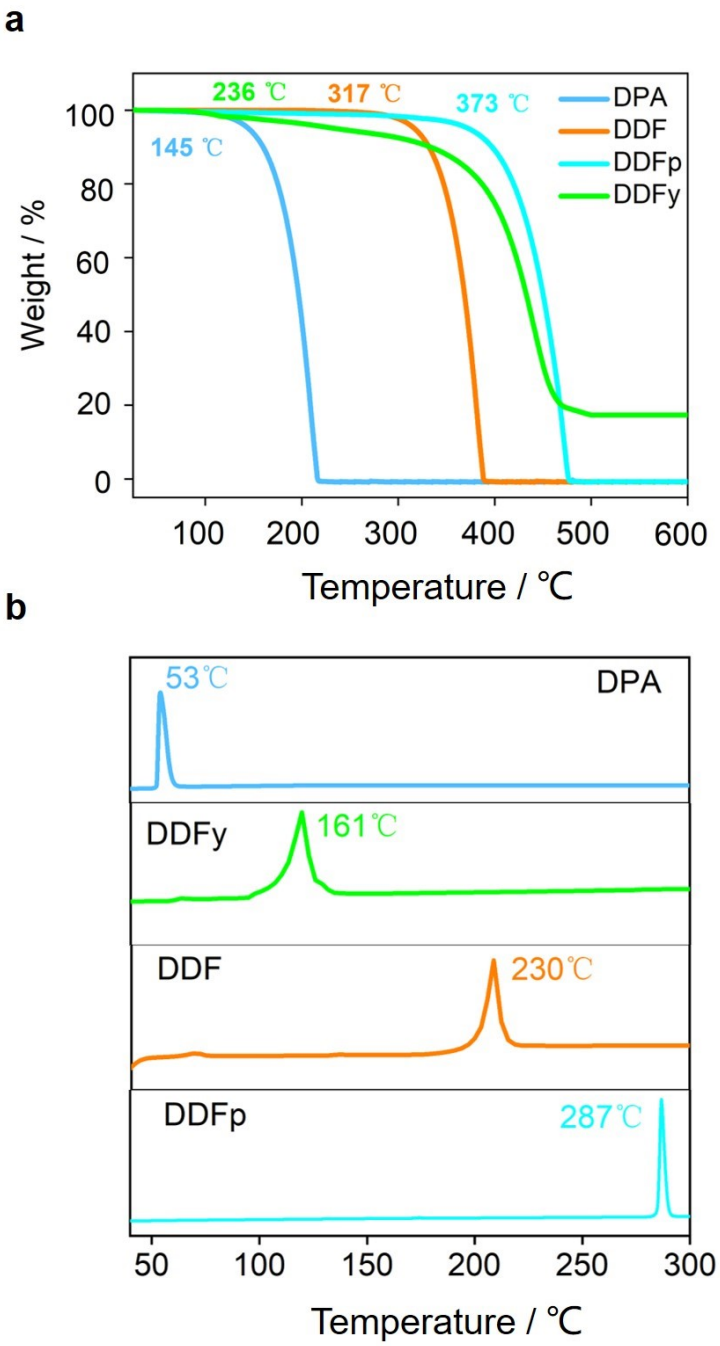

Fig. S1. a) TGA and b) DSC curves of DPA (blue), DDFy(green), DDF (orange) and DDFp (cyan).

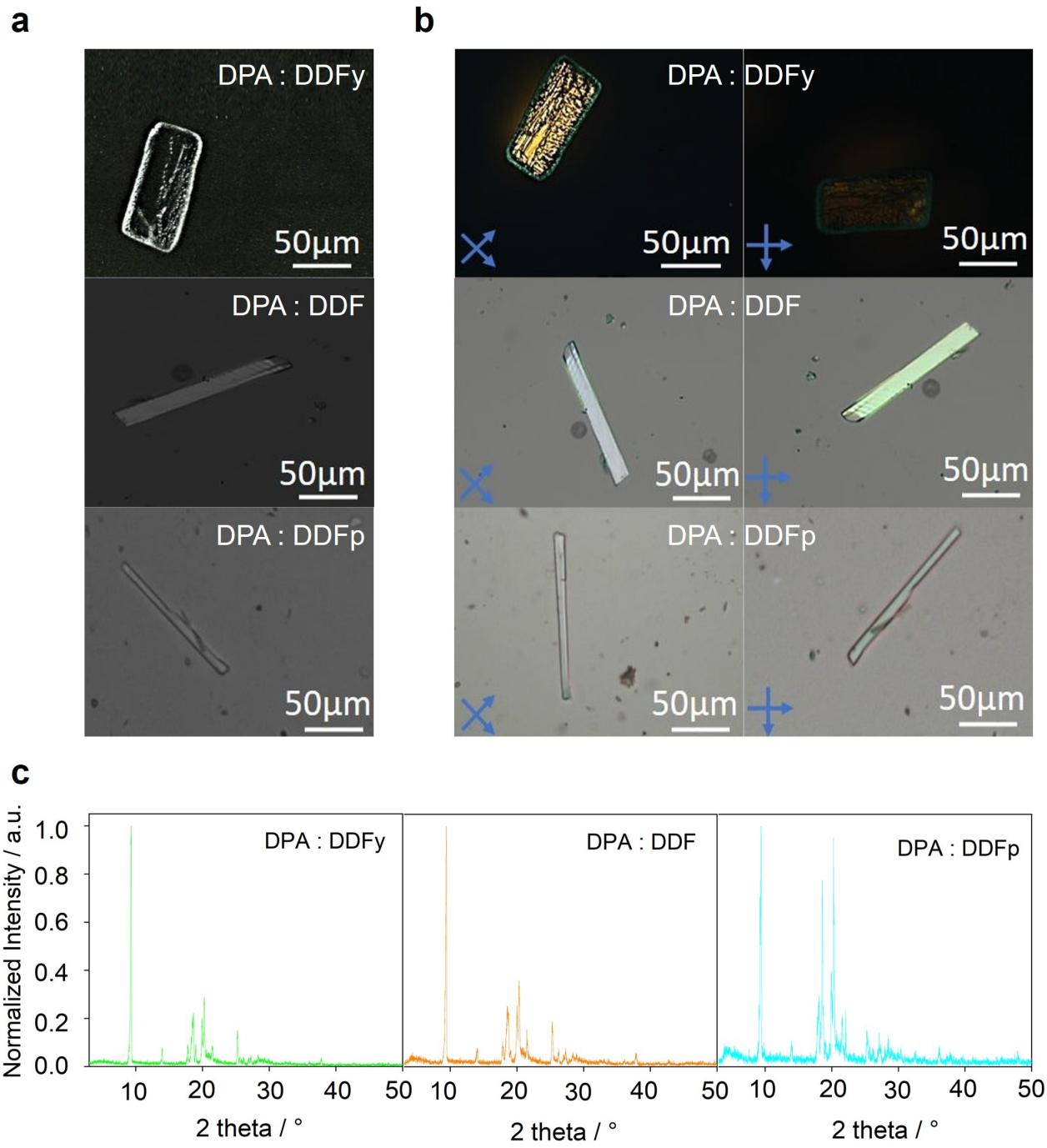

Fig. S2. a) Optical and b) polarized microscope images of the DPA:DDFy (up), DPA:DDF (middle), DPA:DDFp (down) doped-crystals, and the arrows indicating the relative polarizer direction. c) XRD spectra of the DPA:DDFy (left), DPA:DDF (middle) and DPA:DDFp (right) crystals.

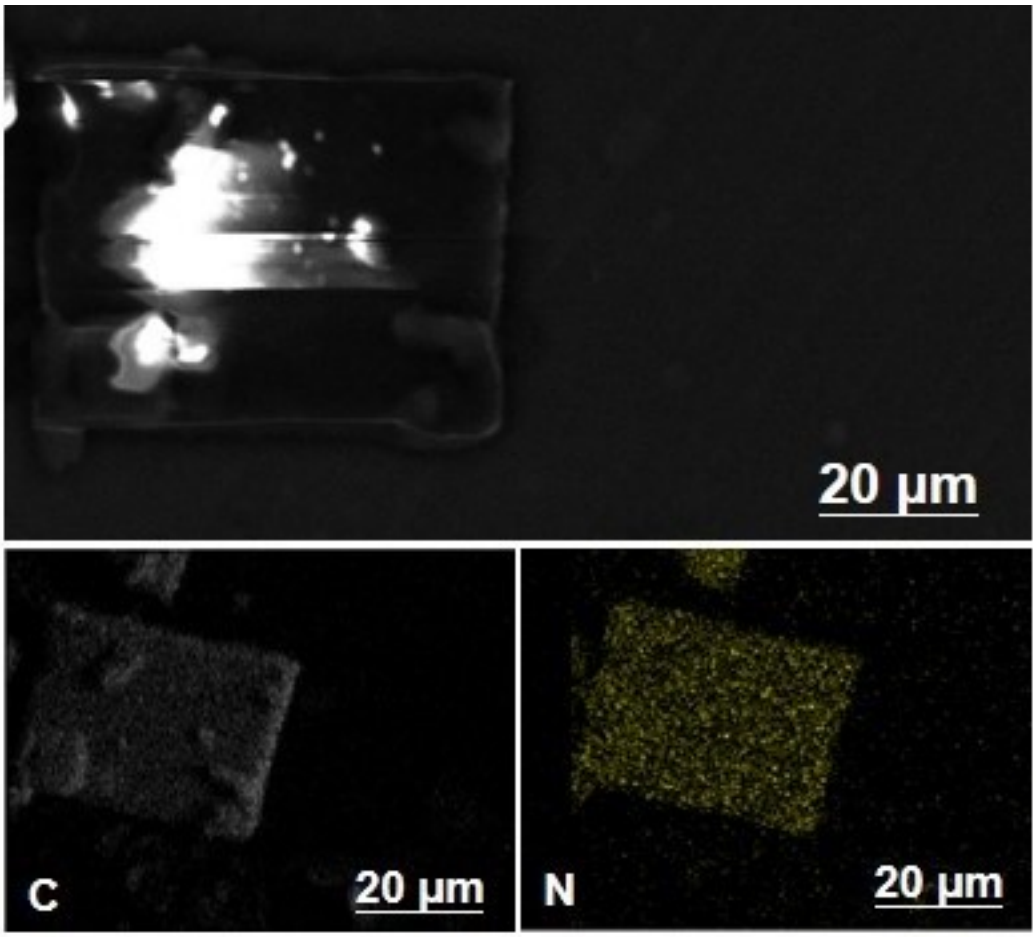

Fig. S3. SEM pictures with the corresponding EDX mappings of the DPA: DDF doped-crystals.

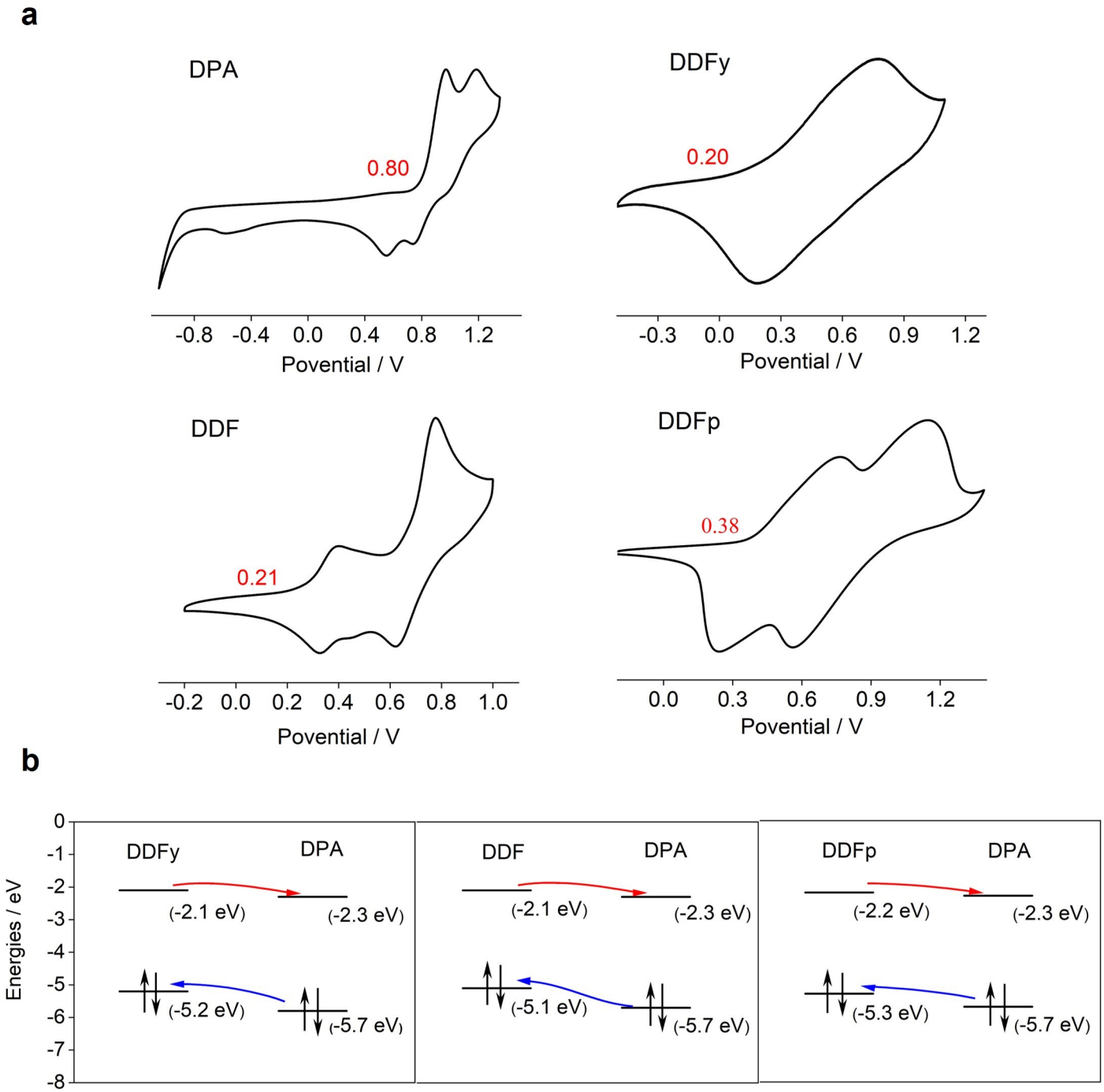

Fig. S4. a) Electrochemical curves of DPA, DDFy, DDF and DDFp in dichloromethane vs Ag/Ag^{+}, with the concentration of 5×10^{-4} mol·L^{-1}. b) Orbital energy levels of DPA, DDFy, DDF and DDFp determined electrochemically, which calculated methods were showed in Table S3. The red and blue lines indicate the possible electron and hole transfer, respectively.

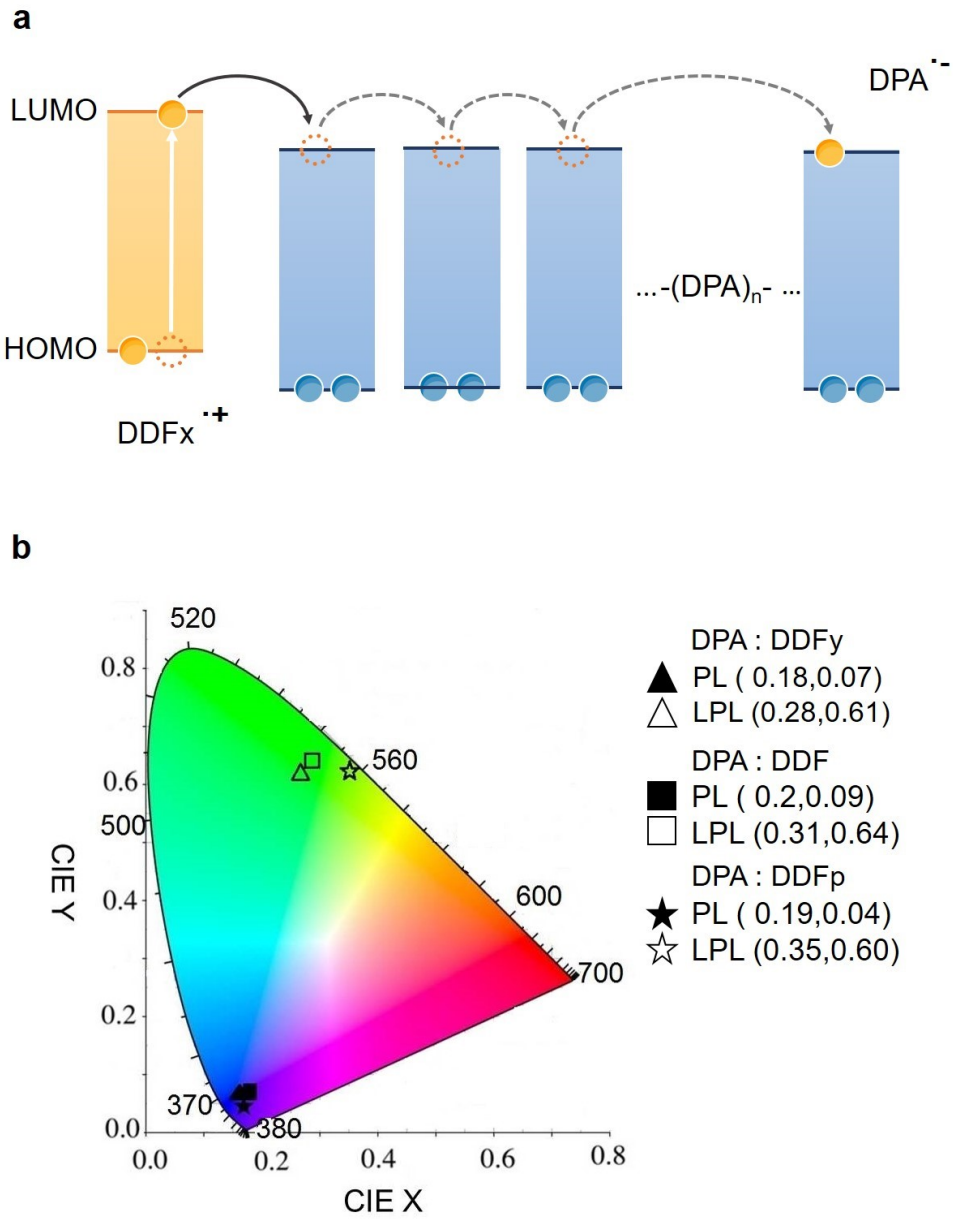

Fig. S5. a) Photo-induced charge separation *via* electron transfer in the doped-crystals DPA:DDF*x* (*x* = y, p or none), and the $(DPA)_n$ (n $\geqslant$ 0) refers to several DPA molecules. b) Emission colors in a CIE 1931 chromaticity diagram: photoluminescence (PL, solid) and LPL (hollow).

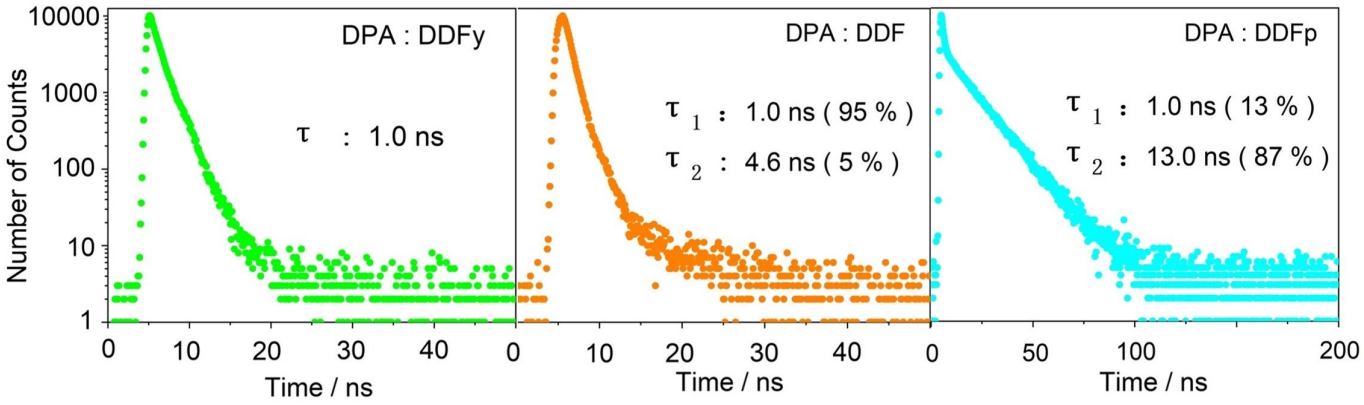

Fig. S6. Fluorescence emission decay spectra of the DPA:DDFy (left), DPA:DDF (middle) and DPA:DDFp (right) doped-crystals (Excitation: 365 nm, Emission: 420 nm).

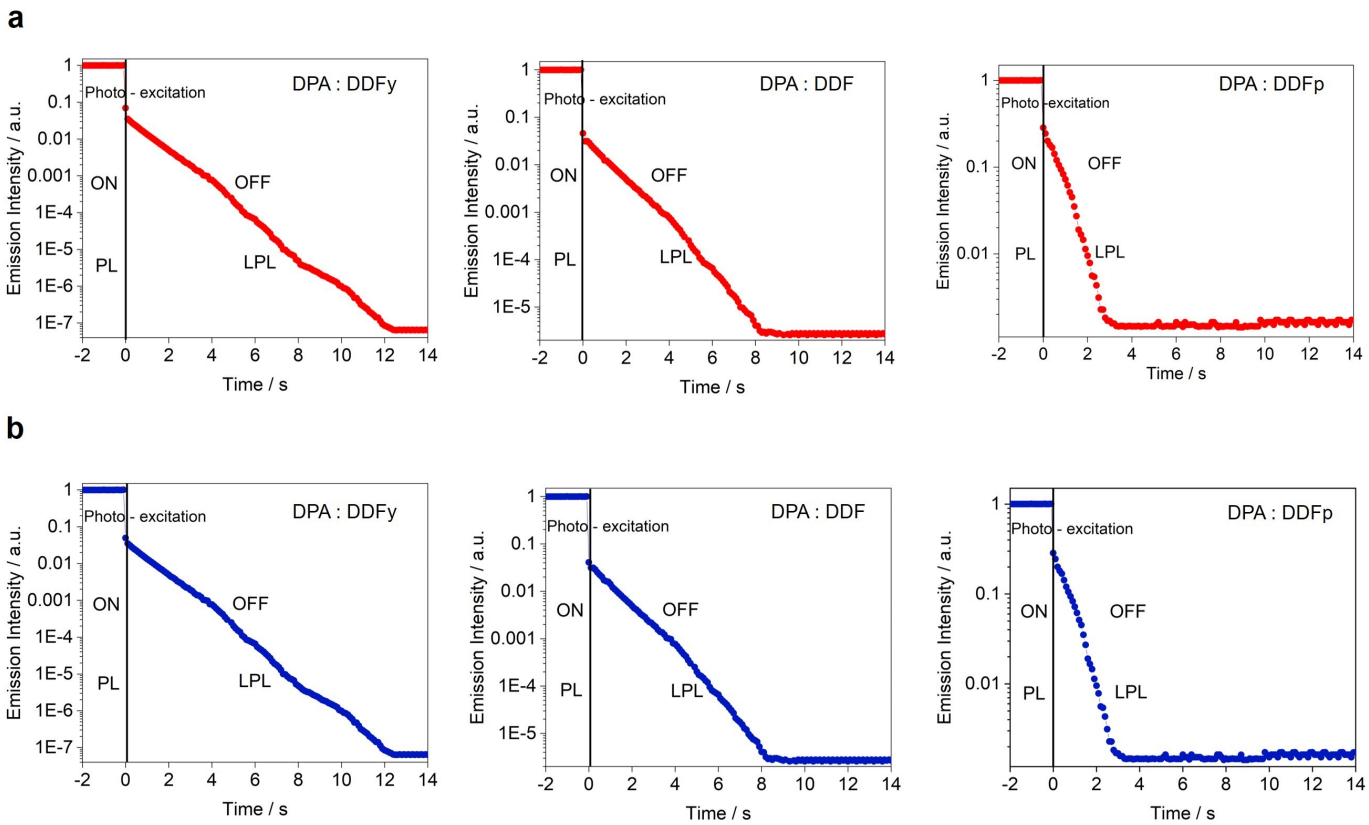

Fig. S7. Semi-logarithmic plot of the emission decay profile of the doped-crystals a) prepared in nitrogen atmosphere and b) placed under water-oxygen conditions for 1 month (excitation wavelength: 365 nm; excitation power: 10 mW; excitation time: 2 s; sample temperature: 300 K).

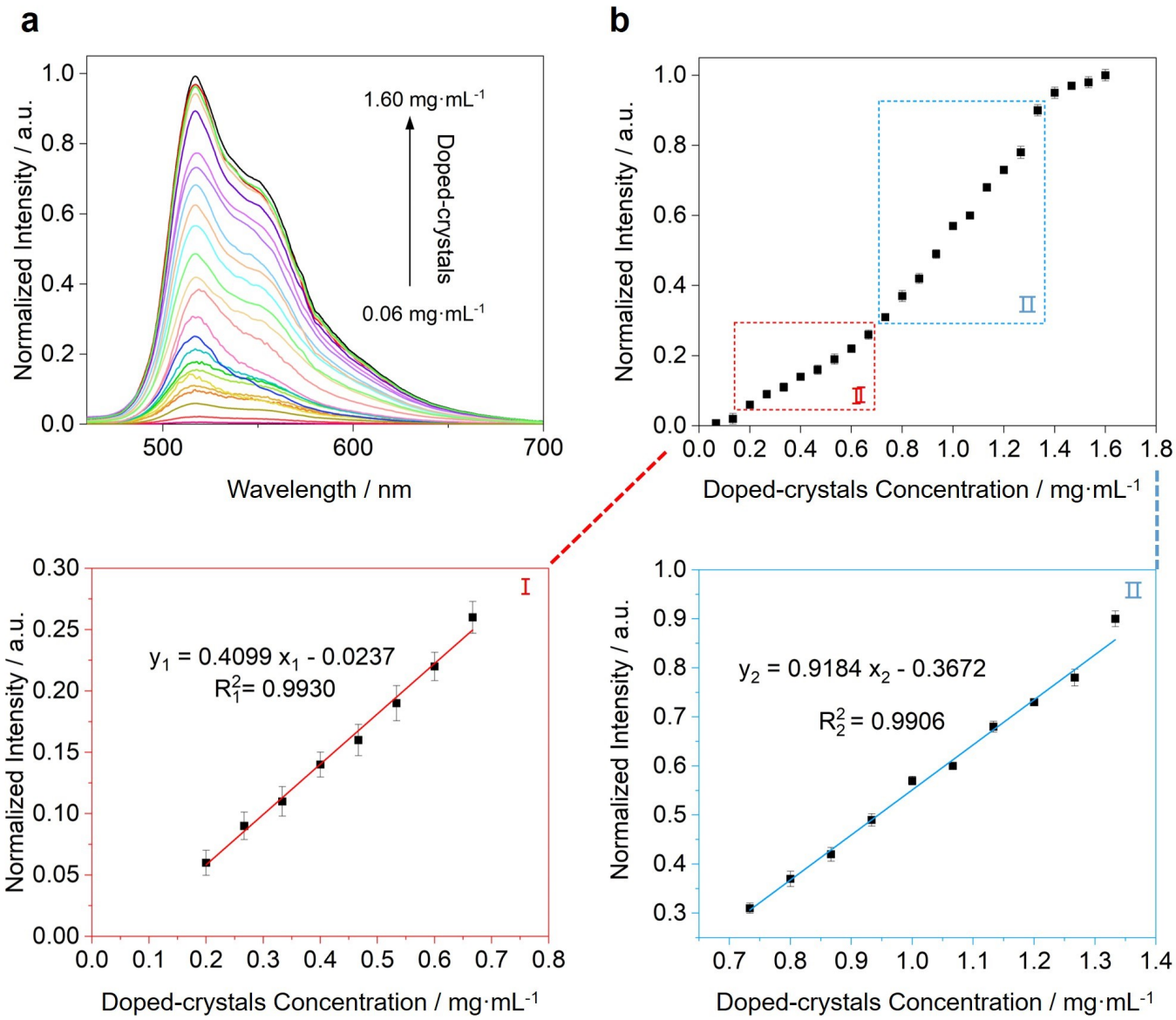

Fig. S8. (a) RTP spectra and (b) Standard curves of different concentration (from 0.06 mg·mL^{-1} to 1.60 mg·mL^{-1}) of the DPA:DDF doped-crystals after interacting with 1.00 mg·mL^{-1} of DNA hydrolysate.

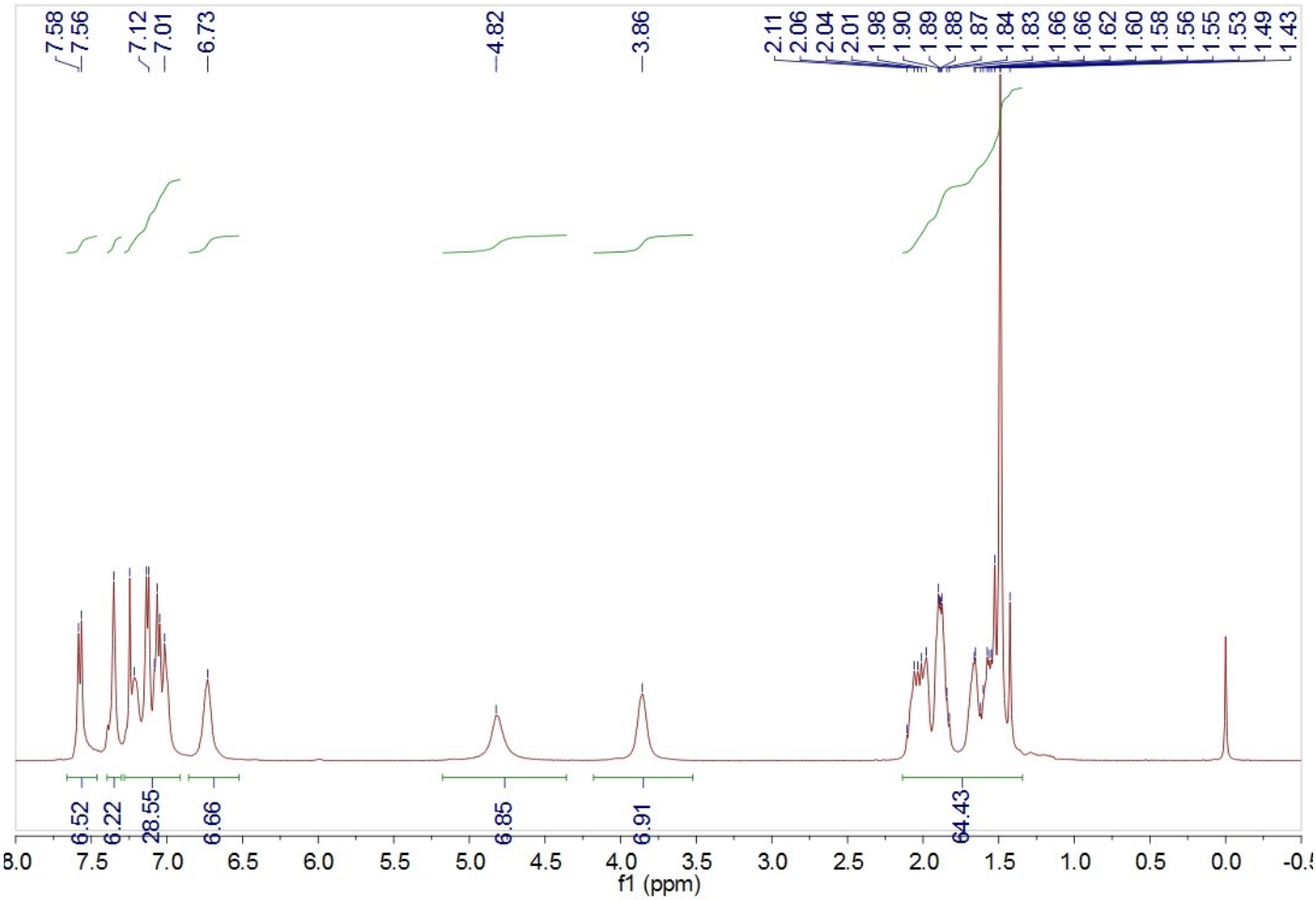

Fig. S9. 400 MHz ^{1}H NMR spectrum of DDFy in $CDCl_3$.

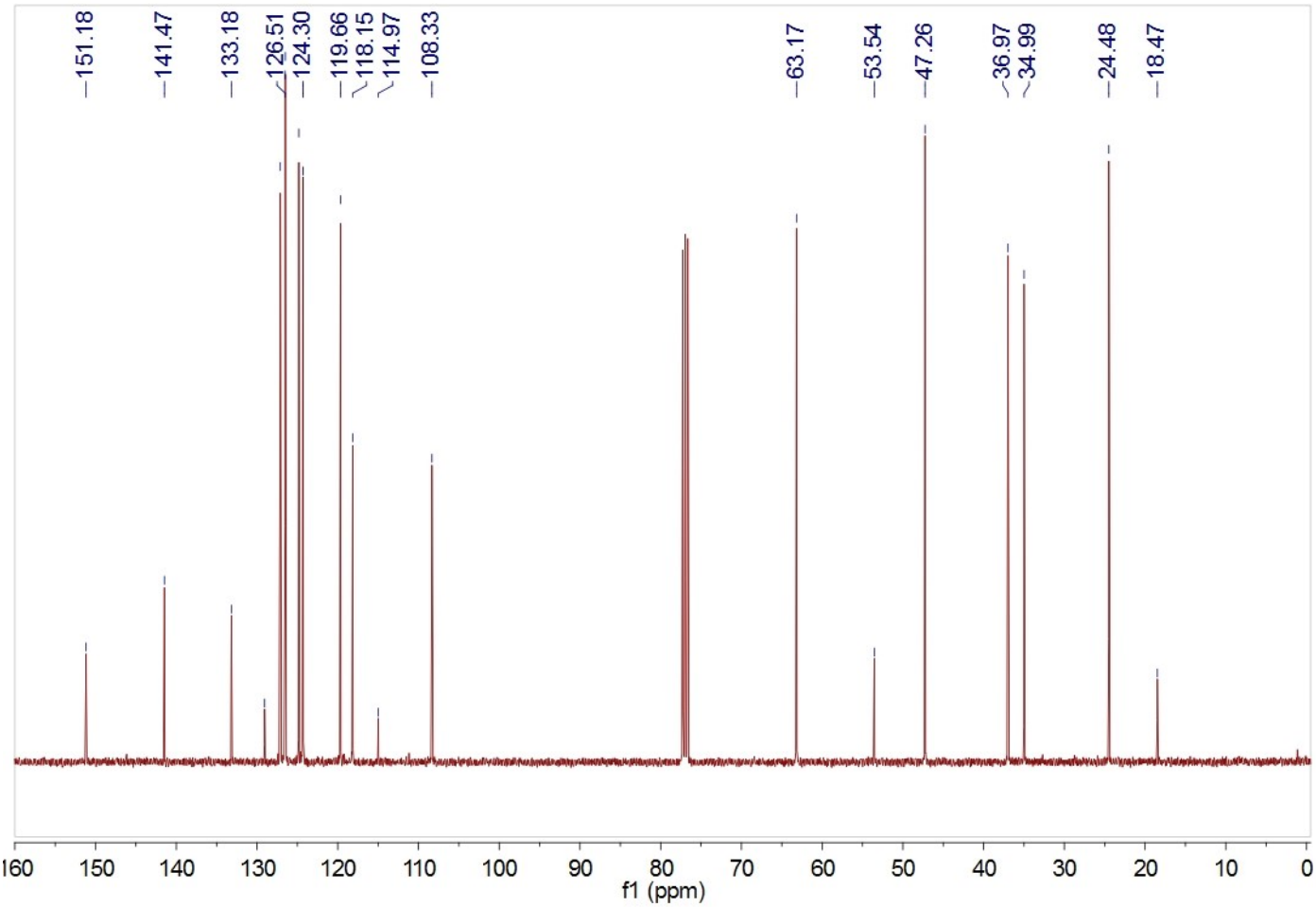

Fig. S10. 100.6 MHz ^{13}C NMR spectrum of DDFy in $CDCl_3$.

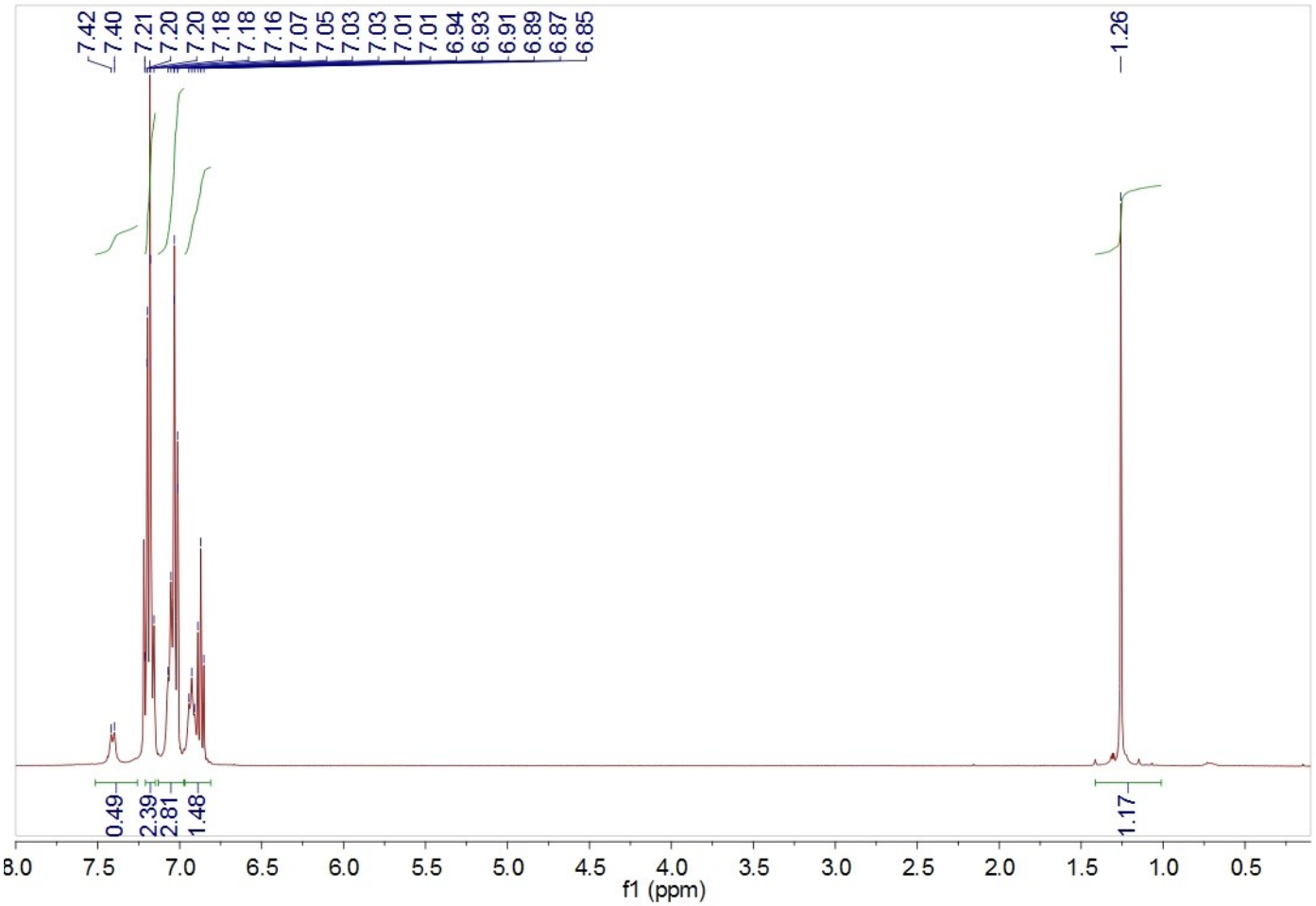

Fig. S11. 400 MHz ^{1}H NMR spectrum of DDF in $CDCl_3$.

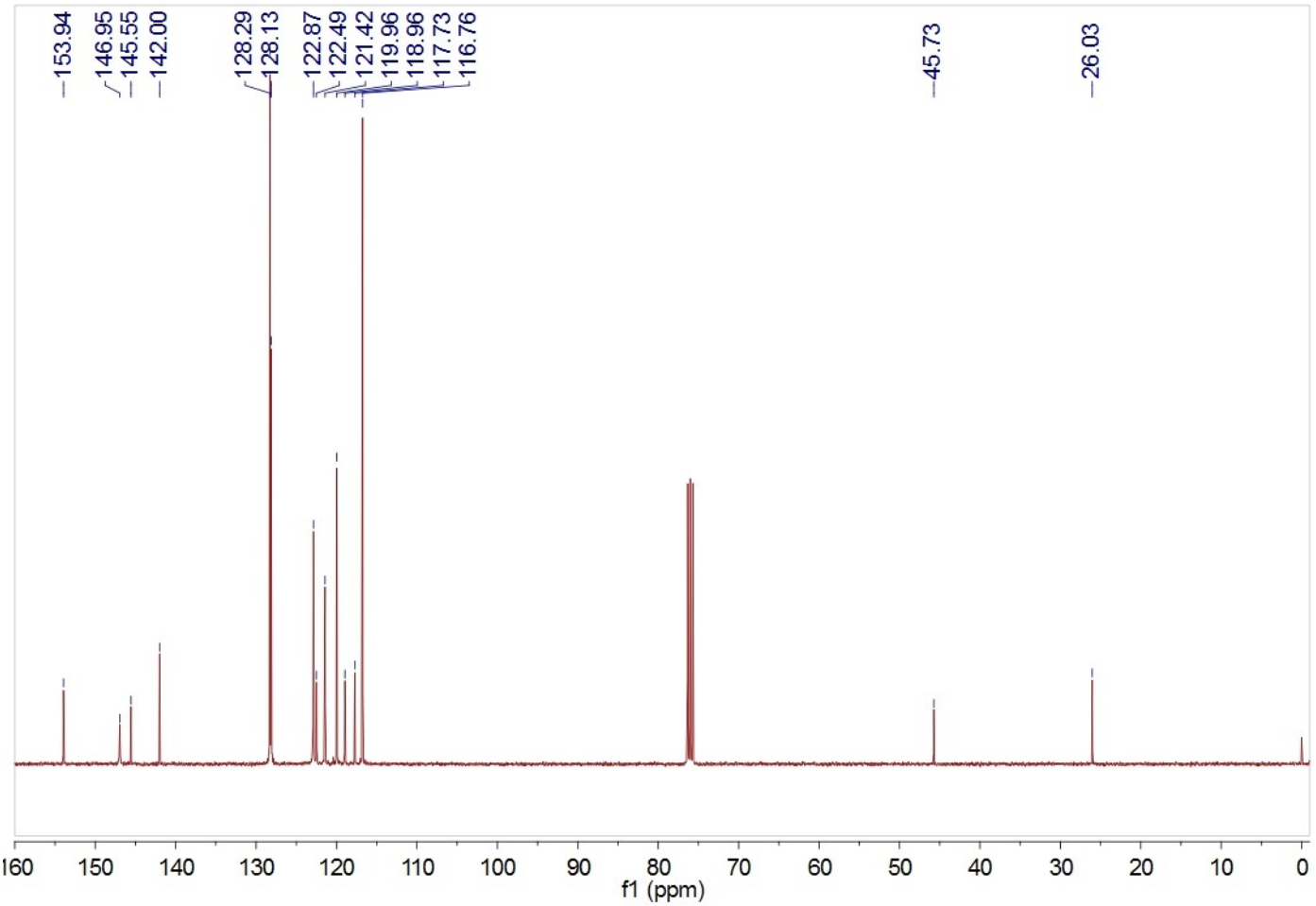

Fig. S12. 100.6 MHz ^{13}C NMR spectrum of DDF in $CDCl_3$.

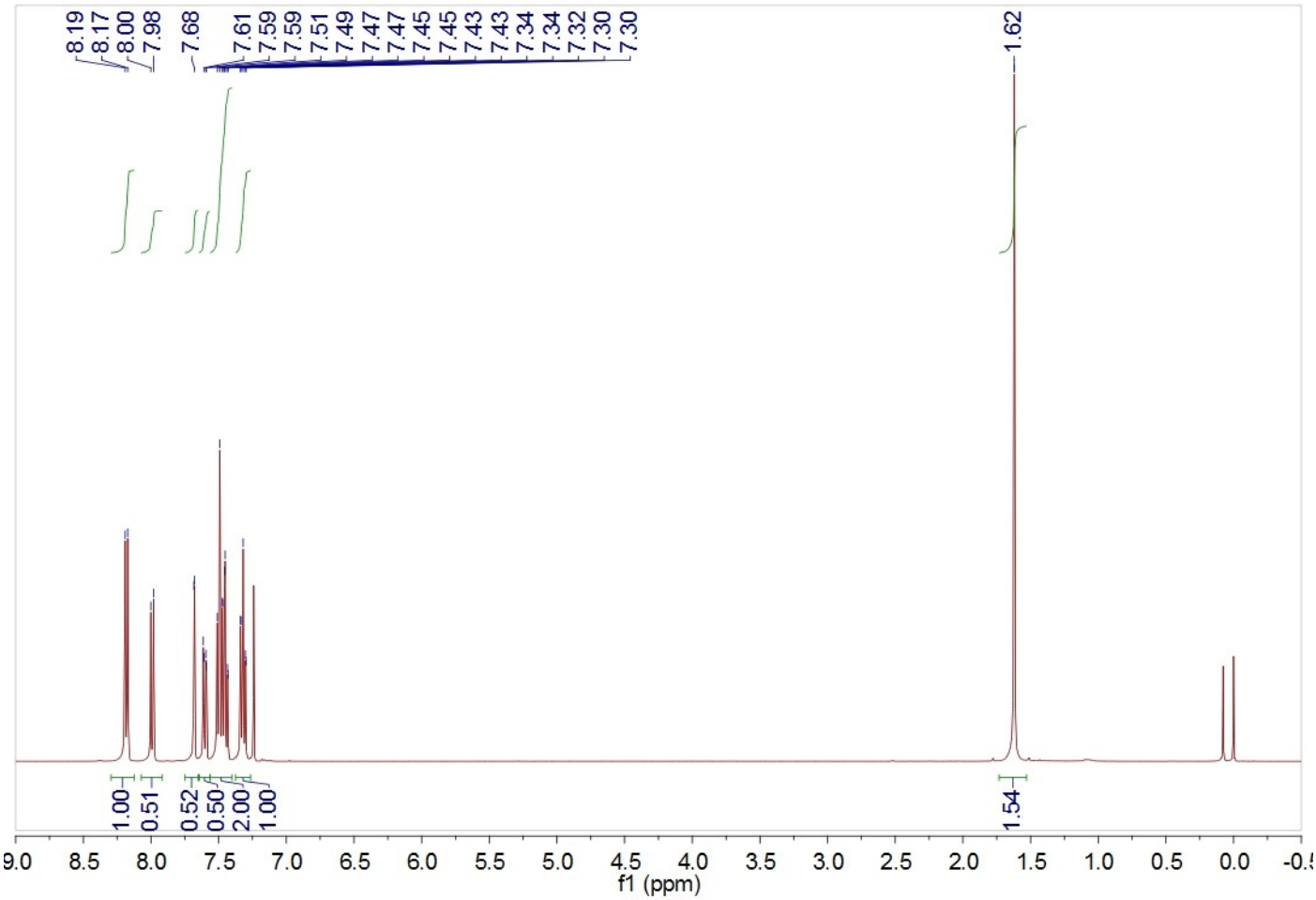

Fig. S13. 400 MHz ^{1}H NMR spectrum of DDFp in $CDCl_3$.

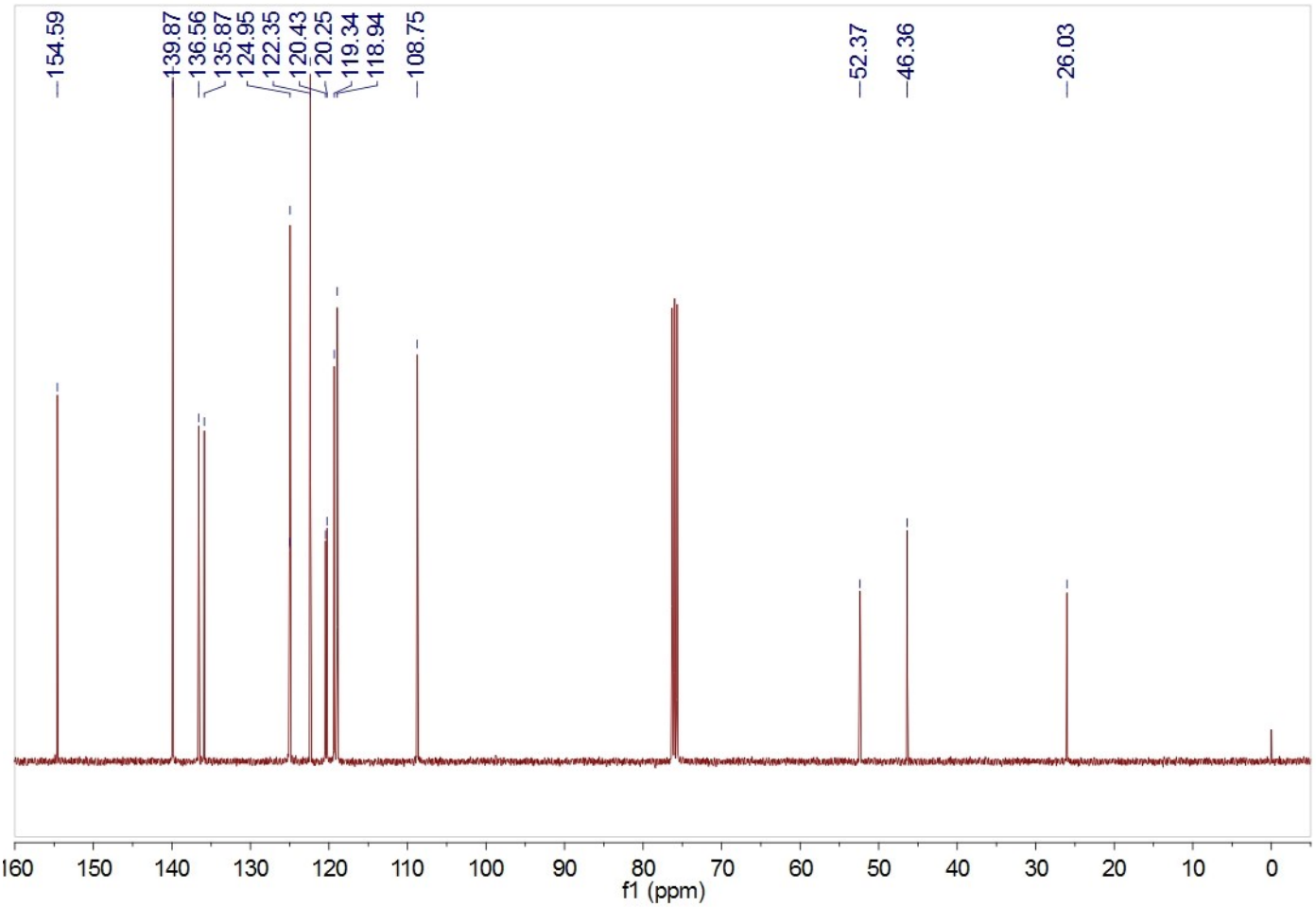

Fig. S14. 100.6 MHz ^{13}C NMR spectrum of DDFp in $CDCl_3$.

References

1 D. Y. Muleta, J. Song, W. Feng, R. Wu, X. Zhou, W. Li, L. Wang, D. Liu, T. Wang and W. Hu, *J. Mater. Chem. C*, 2021, **9**, 5093-5097.

2 J. Song, D. Y. Muleta, W. Feng, Y. Song, X. Zhou, W. Li, L. Wang, D. Liu, T. Wang and W. Hu, *Dyes Pigm.*, 2021, **193**, 109501.

3 J. Han, W. Feng, D. Y. Muleta, C. N. Bridgmohan, Y. Dang, G. Xie, H. Zhang, X. Zhou, W. Li, L. Wang, D. Liu, Y. Dang, T. Wang and W. Hu, *Adv. Funct. Mater.*, 2019, **29**, 1902503.

4 T. Wang, K. C. Weerasinghe, H. Sun, X. Hu, T. Lu, D. Liu, W. Hu, W. Li, X. Zhou and L. Wang, *J. Phys. Chem. C*, 2016, **120**, 11338-11349.

5 T. Wang, C. Zhao, L. Zhang, T. Lu, H. Sun, C. N. Bridgmohan, K. C. Weerasinghe, D. Liu, W. Hu, W. Li, X. Zhou and L. Wang, *J. Phys. Chem. C*, 2016, **120**, 25263-25275.

6 Y. Zhao, S. Xiang, X. Dai and K. Yang, *Appl. Microbiol. Biotechnol.*, 2013, **97**, 5069-5077.

7 A. Lajmi, I. Bourven, E. Joussein, S. Simon, M. Soubrand and M. Mehdioub, *J. Soils Sediments.*, 2019, **20**, 943-950.

8 W. Yun, J. Jiang, D. Cai, P. Zhao, J. Liao and G. Sang, *Biosens. Bioelectron.*, 2016, **77**, 421-427.

9 R. R. Duan, L. Wang, W. Q. Huo, S. Chen and X. H. Zhou, *Spectrochim. Acta A Mol. Biomol. Spectrosc.*, 2014, **128**, 614-621.

10 S. Yatsushiro, Y. Yamaguchi, S. Yamamura, Y. Shinohara, Y. Baba and M. Kataoka, *J. Pharmaceut. Biomed.*, 2011, **55**, 202-205.

11 L. Yi, H. Zhao, C. Sun, S. Chen and L. Jin, *Spectrochim. Acta A Mol. Biomol. Spectrosc.*, 2003, **59**, 2541-2546.

12 Y. Zhao, L. Liu, H. Kuang, L. Wang and C. Xu, *RSC Adv.*, 2014, **4**, 56052-56056.

13 Q. He, D. Yu, M. Bao, G. Korensky, J. Chen, M. Shin, J. Kim, M. Park, P. Qin and K. Du, *Biosens. Bioelectron.*, 2020, **154**, 112068.

14 Z. Li, H. Xu, S. Li, S. Wu and X. Miao, *Anal. Chim. Acta*, 2021, **1159**, 338428.

15 I. D. Podmore, D. Cooper, M. D. Evans, M. Wood and J. Lunec, *Biochem. Biophys. Res. Commun.*, 2000, **277**, 764-770.

16 D. H. Kang, Y. Zeng, M. Tewari and J. Kim, *Biosens. Bioelectron.*, 2022, **199**, 113889.

17 T. Arslan and O. Guney, *Anal. Biochem.*, 2020, **591**, 113540.

18 J.-M. Liu, T.-L. Yang, F. Gao, L.-X. Hu, H.-X. He, Q.-Y. Liu, Z.-B. Liu, X.-M. Huang and G.-h. Zhu, *Anal. Chim. Acta*, 2006, **561**, 191-197.

19 Y. D. Zhang, Y. Wu, Y. Xu, Q. Wang, K. Liu, J. W. Chen, J. J. Cao, C. Zhang, H. Fu and H. L. Zhang, *J. Am. Chem. Soc.*, 2016, **138**, 6739-6745.